actuators

MDPI

Article

Foot Drop Stimulation via Piezoelectric Energy Harvester

Parham Soozandeh [1], Ganga Poudel [2], Morteza Sarkari [2] and Kamran Behdinan [1,*]

[1] Department of Mechanical and Industrial Engineering, University of Toronto, Toronto, ON M5S 3G8, Canada; parham.soozandeh@mail.utoronto.ca
[2] Institute of Biomedical Engineering, University of Toronto, Toronto, ON M5S 3G9, Canada; ganga.poudel@mail.utoronto.ca (G.P.); m.sarkari@mail.utoronto.ca (M.S.)
* Correspondence: behdinan@mie.utoronto.ca

Abstract: The design and implementation of a piezoelectric energy-harvesting system, aimed at stimulating the Tibialis anterior muscle to aid patients struggling with a foot drop disability, are investigated. A physical prototype designed to be installed inside a shoe sole, consisting of an energy-harvesting unit along with a power-management circuit and a functional electrical-stimulation circuit, is fabricated. The piezoelectric energy harvester (PEH) incorporated six layers of Polyvinylidene-Fluoride sheets to achieve a mean-charge generation of 65.25 μC/step and a peak power of 10.76 mW/step. A peak voltage of +80.0 V generation was achieved during a stomping motion. The electrical systems store, convert, and deploy 60 mA electric pulses at the desired frequencies to the target muscle. The finalized prototype is best-suited to prolong the duration of the charged batteries whilst in use. In a practical sense, it should be used alongside external-power sources to recharge the batteries installed in a foot drop stimulation device. The PEH in its current state is fully capable of solely powering blood pressure sensors, glucose meters, or activity trackers.

Keywords: wearable piezoelectric energy harvester; biomedical; foot drop; stimulation; shoe sole; functional-electrical stimulation; power-management circuit

Citation: Soozandeh, P.; Poudel, G.; Sarkari, M.; Behdinan, K. Foot Drop Stimulation via Piezoelectric Energy Harvester. *Actuators* **2022**, *11*, 174. https://doi.org/10.3390/act11070174

Academic Editor: Hongli Ji

Received: 29 May 2022
Accepted: 20 June 2022
Published: 22 June 2022

1. Introduction

With sustainability becoming a major, global focus point, it is ever more critical to find methods through which energy production and consumption can become more environmentally friendly. A key method to minimize wasted or unutilized energy is to harvest energy where possible, store it, and deploy it when needed. Energy harvesting via piezoelectric materials is one method to reduce the reliance on batteries in the future. The field of medical devices is one such area that can greatly benefit from such innovations to improve the lives of patients and alleviate the difficulties caused by their medical conditions. This paper is focused on bridging the literature gap surrounding the unexplored biomedical-application potential of energy harvesters, in aiding patients suffering from foot drop. A novel-stimulation system consisting of a shoe-mounted piezoelectric energy harvester (PEH), working in tandem with a Functional Electrical-Stimulation (FES) system, has been designed and fabricated to aid patients suffering from this underlying neurological or muscular disability.

FES is a very prominent medical-device application that allows for movement restoration in patients with nerval or muscular damage. FES works by activating healthy neuromuscular tissues beneath the damaged site, resulting in muscle contractions that help with the function of the paretic limbs [1]. Foot drop is one of the pathologies in hemiplegic patients and indicates insufficient dorsiflexor-muscle activation due to underlying muscular or neurological disorders. Foot drop can be classified as when the foot can no longer be actively lifted when taking steps [2]. Such impairments cause difficulties with performing day-to-day activities and reduce mobility, thereby reducing the quality of life for the patient.

FES basically mimics the normal function of the peroneal nerve and helps the patient contract the Tibialis anterior (TA) muscle to lift the forefoot while walking [3]. An alternative to using an FES system for foot drop is to use an ankle–foot orthosis, which is a brace that is worn to help with the posture and support of the foot muscles. A study by Karniel et al. [4] found that both methods delivered satisfactory rehabilitation results in the long term. Patients using FES systems recorded significant improvement in their gait after 4 weeks, whilst it took the ankle–foot orthosis patients 12 weeks to show significant improvements.

The proposed solution in this paper is to harvest energy from the human body by placing a PEH within the shoe soles of the patient thereby utilizing the large compressive force of the heel strike. Figure 1 shows an overview of the system during a typical human-gait cycle. During the first stage of the gait cycle when the heel strikes the ground, a foot switch within the shoe sole is pressed, thereby initiating the process of energy harvesting. During the second stage or stance, a significant amount of pressure is exerted on the harvester, thereby generating electrical energy. This energy is stored in the Power Management Circuit (PMC) for later deployment. Each time the affected heel is then raised, the foot switch is triggered thereby releasing the stored energy through the FES circuit and into the electric pads, which are placed on the TA muscle. This causes contraction of the muscle and raises the affected feet during the swing stage of the gait cycle. The cycle repeats when the patient takes the next step. The design of the PEH allows for high rates of deformation and, thus, energy generation.

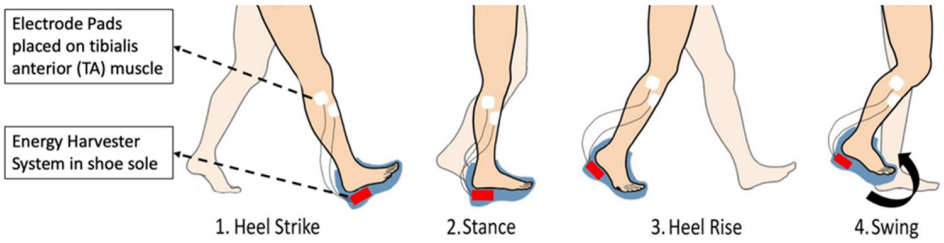

Figure 1. Visualization of the energy-harvesting system within the human-gait cycle.

In a paper by Kim et al. [5] a piezoelectric sensor was developed using boron nitride nanosheets (BNNS). This allowed them to produce a transparent and flexible sensor, which once combined with PDMS for increased flexibility, allowed for maximum contact with the human skin. Electrical signals were able to be detected from the movements in the human foot, neck, and legs. In a paper by Zurbuchen et al. [6], an implantable energy harvester (EH) was designed by modifying the quartz watch's mechanism and sewing it onto a sheep's heart to harvest electrical energy from the movement of the heart. In that research, the observed output was in the range of 10–90 μW depending on the size of the EH. In a paper by Hinchet et al. [7], an EH was implanted under the skin of a pig to harvest energy from external ultrasonic sources to produce 6.24 V and 200 μA. Alam et al. [1] performed a study on transcutaneous nerve stimulation of the surrounding muscles of a rat's spine. The EH worked via acoustic-energy transfer, which once implanted 8 mm beneath the skin, could generate an output of 5.95 mW with an acoustic intensity of 379.92 mW/cm^2. A PEH to be implemented inside of a shoe sole was developed by Jeong et al. [8], which featured a spring and cantilever setup. This prototype generated 52 μW and was used to power a wireless transmitter to detect emergency accidents for people working during the night in remote places. Yin et al. [9] undertook a more complex shoe-mounted PEH design, which featured gears, axles, bearings, and springs to bend two piezoelectric beams during the gait cycle. Their prototype achieved a peak power output of 9.17 mW at 1.5 Hz frequency and a mean power output of 0.11 mW. A ferromagnetic ball and cantilever setup was pursued by Fan et al. [10], which was used to generate electricity from the vibrations caused by the foot during walking. This shoe-mounted PEH achieved a peak power of 0.35 mW at 8 km/h walking speed. Other mechanism can be pursued to harvest energy, such as the rotary motion developed by Narolia et al. [11]. As the chosen application would benefit

from fast-charging and discharging rates, more advanced materials such as the sodium bismuth niobate ceramics explored by Manan et al. [12] can be beneficial as well. Every component of an EH system can be optimized to harvest the maximum amount of energy from a given excitation. Chebanenko et al. [13] developed a suitable optimization technique for cantilever style structures, to be used inside EH systems.

Conventional FES systems used bulky step-up transformers and switched the MOSFET in their output-driver stage. However, this resulted in monophasic, unbalanced anodic/cathodic charge, a large rise and fall time of stimulation pulses, line-frequency noise causing unwanted high-voltage spikes in the output, and distorted morphology of the pulses [14,15]. These issues led to the inappropriate firing of neurons or excessive excitability of neurons, resulting in more muscle fatigue, tissue damage, or insufficient dorsiflexion from inconsistent motor-unit recruitment. Ideally, FES devices for foot drop need to produce a rectangular charge-balanced biphasic waveform, which is considered safe and efficacious [14]. In addition, this waveform optimally activates muscles, thereby reducing the stimulated muscle fatigue. As a solution, Cheng et al. [16] first proposed DC–DC architecture to boost the voltage instead of using the transformer-MOSFET design. Shendkar et al. [14] later designed an FES device named 'InStim', using a similar DC–DC-architecture design. This paper took inspiration from this 'InStim' device and designed a custom FES system with significant modifications.

2. Materials and Methods

The electrical system of our design consists of a PMC demo board and an FES system. PMC demo board and FES Printed Circuit Board (PCB) are used to take the charge from the PEH and output the balanced, biphasic high-voltage, and high-current pulses for surface neural stimulation.

2.1. Power-Management Circuit (PMC)

A PMC is required to accumulate the charge from the piezoelectric sheets, store the harvested energy in the external storage capacitor, and convert that energy into a useful voltage. For this paper, the piezoelectric energy-harvesting power-supply demo board from Analog Devices, Inc.™ is being used as the PMC. This circuit consists of a highly efficient buck DC–DC converter to harvest electrical energy and convert it into a well-regulated output of 3.3 Volts. The charge accumulates on an input capacitor until the buck converter can efficiently transfer some of the stored charge to the output [17,18]. The buck converter also delivers up to 100 mA of continuous output current alongside the output of 3.3 Volts [17].

2.2. FES System

We adopted coupled inductor-based DC–DC boosters and low-current output driver-stage topology for our FES system [14]. A DC–DC voltage booster and a high-power current-source op-amp are the two main components of this system, allowing the device to deliver biphasic pulses of high-voltage and constant current. The charge from the PEH goes into the PMC board, where this charge gets converted into 3.3 V. The 3.3 V output is then provided as the input to the microcontroller and the DC–DC-boost converters. The monophasic pulses from the microcontroller are fed into the converter to generate biphasic pulses. The output driver takes in the biphasic waveforms and high voltage to convert them into constant current. This current is then applied to the patient using the stimulation electrodes. These electrodes are stimulated based on the biofeedback of the patient using the tactile-switch sensor.

2.2.1. Microprocessor Unit

The microprocessor (MSP430F131IPWR; Texas Instruments Inc.™, Dallas, TX, USA) was used to generate a sequence of pulses. This microprocessor generates two independent

monophasic pulses with +3.3 V amplitude. These pulses are then transmitted to the biphasic-pulse converter.

2.2.2. Biphasic-Conversion Unit

This converter unit receives monophasic pulses from the microprocessor and converts them into the biphasic waveforms. This is done with two operational amplifiers (TLV2374IDR; Texas Instruments Inc.™, Dallas, TX, USA), with one acting as the differential amplifier and the other as the buffer for impedance matching.

2.2.3. DC–DC-Boost Converters

Since only a peak-to-peak pulse of 100 V or higher can provide suitable ankle dorsiflexion in patients with foot drop, boost converters are required to boost the voltage [14]. Two DC–DC-boost converters (TPS61170; Texas Instruments In.™, Dallas, TX, USA) are used with the coupled inductors (LPR4012-103D; CoilCraft Inc.™, Cary, IL, USA), to boost the voltage to around 70 V [14,19]. These boosted voltages are provided to the output driver as the high-voltage positive (+70 V) and negative rails (−70 V).

2.2.4. Output Driver

The output driver uses a high-voltage to high-current converter operational amplifier (PA441DF; Apex Microtechnology™, Tucson, AZ, USA). This driver op-amp uses an external resistor to limit the current for patient safety. The maximum-current limit was kept at 60 mA, with a current-limiting resistance of 10 ohms [17,19]. With the maximum-current limit of 60 mA, the output voltage needed was calculated to be 120 V, using the skin resistance of 2 kΩ [14,15].

2.2.5. Biofeedback

A tactile-switch sensor (GT-TC089A-H085-L1; LCSC™, Shenzhen, China) is used to record the gait cycle of stroke patients. This sensor will be placed under the heel of the shoe sole worn on the hemiplegic foot [14]. When the patient lifts their leg for walking, the foot switch turns off and the microprocessor receives feedback from the sensor. The microprocessor then generates stimulation pulses, but when the patients place their foot on the ground, the switch turns on. This event then triggers the microprocessor to turn the stimulation pulses off.

Figure 2 shows our complete FES board, which was designed by us and custom-ordered from JLCPCB™, along with the tactile switch. A tactile switch was directly placed on the FES board to make the process of conducting multiple performance tests of this board easier. However, as this board is large and bulky, it is not deemed practical to insert into the insole of a shoe for real-world application. To overcome this problem, we designed a small PCB board with a tactile switch, which could be inserted into the insole of the shoe of a stroke patient. The tactile-switch output from this small PCB board will then be connected to the FES board, using electrical wires to control stimulation pulses from the microprocessor.

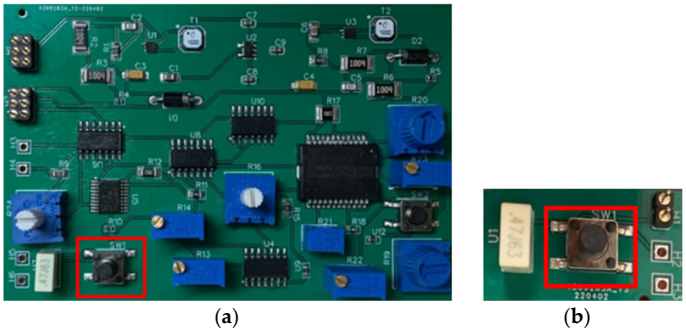

(**a**) (**b**)

Figure 2. (**a**) FES circuit board with red box around the tactile switch; (**b**) small PCB board with red box around the tactile switch.

2.3. Energy Harvester Assembly

The chosen design assembly consists of three components: bottom plate, top plate, and the border, as depicted in Figure 3. Based on measurements performed on a size 10 male shoe, the available workable area was approximately 110 mm by 70 mm. The mechanism used to deform the piezoelectric sheets was inspired by the work of J. Zhao and Z. You [20]. However, details of the structure's geometry, design, and assembly were modified for this work to suit the intended application. The main purpose of the EH assembly is to distribute the input force to cause high levels of stress and strain on the piezoelectric sheets, without plastic deformation under normal use. This is achieved by the crests and troughs on the top and bottom plates, respectively, which are the inverse of each other, thus allowing the two plates to sit flush when pressed together.

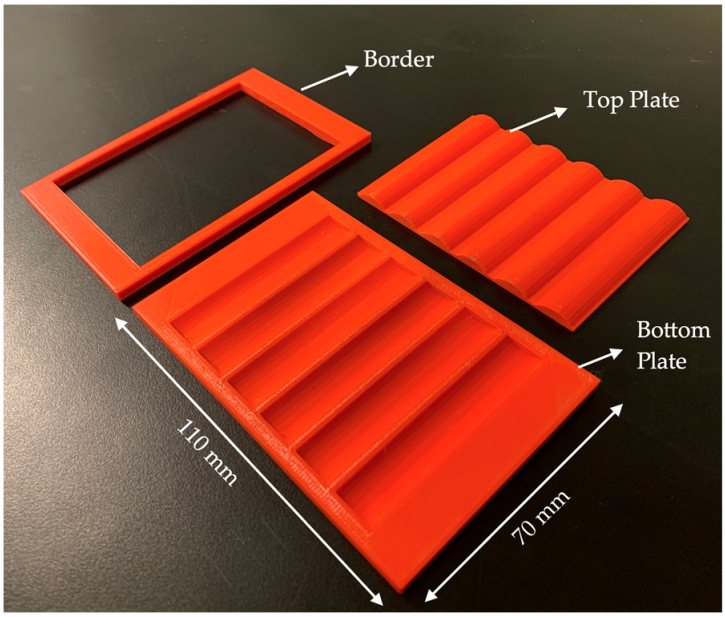

Figure 3. PEH housing-assembly components.

As can be seen from Figure 3, the assembly housing measures 110 mm × 70 mm, with an opening of 80 mm × 60 mm for the upper plate to be secured yet able to travel vertically, upon force input. The assembly housing was fabricated via filament-extrusion 3D printing, using Polylactic Acid (PLA) with 80% cubic infill using the Prusa Research™ MK3 printer. To achieve smooth surfaces on the two plates, a 0.4 mm nozzle was used to reduce sharp edges in between layers, which could lead to the piezoelectric films getting punctured upon force input.

Table 1 outlines the material properties of the Polyvinylidene-Fluoride (PVDF) sheets that were purchased from PolyK Technologies LLC and used in the prototype [21]. Six layers of PVDF were connected in parallel and positioned in between the top and bottom plates. An oscilloscope was used to measure the voltage readings from test runs on the prototype.

Table 1. Material Properties of PVDF Sheets [21].

Material Property	Symbol	Value
PVDF layer thickness	h	100 μm
Electrode (Al) thickness	h_e	50 nm
Dielectric constant	ε	12.5
Piezoelectric constant	d_{31}	31 pC/N
Piezoelectric constant	d_{33}	25 pC/N
Elastic modulus	Y	2700 MPa

The PVDF sheets were cut to the desired size, and their geometrical design parameters along with those of the PEH assembly are outlined in Table 2. These values will be used to conduct an analytical analysis to calculate the charge accumulation by the PEH. These design parameters are also used to model the system via COMSOL® to simulate the loads and validate the experimental observations.

Table 2. Energy-Harvester-Design Parameters [21].

Design Parameter	Description	Value
l	PVDF-layer length	100 mm
w	PVDF-layer width	60 mm
A_s	PVDF-sheet surface area	6.50×10^{-3} m^2
A_{cs}	PVDF-sheet cross-sectional area	6.50×10^{-6} m^2
L	Chord length of crest/trough	12 mm
N	Number of PVDF layers	6
2α	Contact angle of the plates	20°
n	Number of crests/troughs	6

3. Results

The completed prototype was connected to PMC and the FES circuit, leading onto electrode pads that will be placed on the TA muscle for electrical stimulation. In order to conduct experimental analysis on the prototype, the electrode pads were removed, and the endpins were connected to a Tektronix® Mix Domain Oscilloscope (MDO-3024) to measure peak voltage. Figure 4 depicts the completed prototype with all of the circuitry connections.

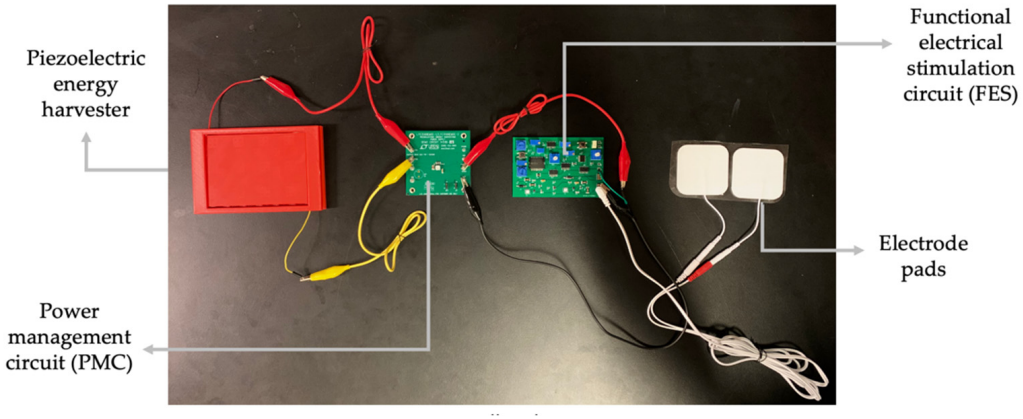

Figure 4. Full-scale prototype components.

3.1. Experimental Results

Oscilloscope Readings

Several experimental runs were conducted on the oscilloscope to assess the performance of the system. Firstly, the wires leading to the electrode pads were connected to the oscilloscope, and a compressive load of 950 N was imposed on the PEH, by having a male participant, weighing approximately 97 kg, stepping with their heel on the top plate at the average walking pace. As can be seen from Figure 5, a peak-to-peak voltage of 3.36 V was observed, as limited output from the PMC, whilst the remaining electrical charge was being used to charge the capacitor on the PMC.

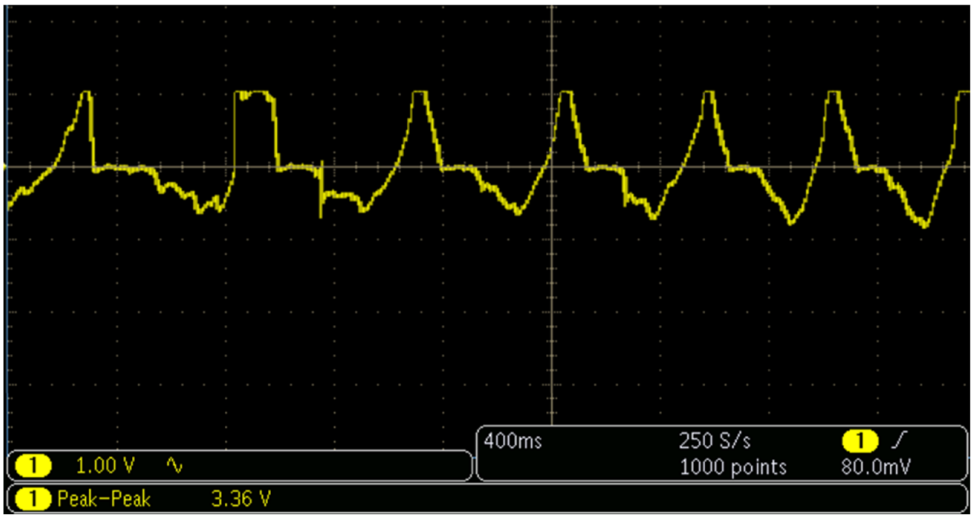

Figure 5. Output voltage under operating condition.

What can be inferred from Figure 5 is the reliability of the prototype in generating consistent signals with each heel strike, and the ability of the PMC circuit to limit the output voltage at the desired 3.3 V. In order to assess the peak voltage of the PEH on its own, the circuitry was disconnected and the PEH was connected directly to the oscilloscope. As shown in Figure 6, the generated voltage exceeded the upper limit of the oscilloscope; even so, a very impressive potential difference of 80.0 V was recorded by a stomping force on the top plate.

Figure 6. Output voltage under stomping motion.

3.2. Analytical Analysis

The compressive force delivered by the top plate during a heel strike is labeled as F_{hs}, responsible for deforming the piezoelectric sheets. For simplicity, it is assumed that F_{hs} can be equally divided among each of the contact points of the crests and troughs, thus, the force at each intersection can be labeled as F_1. The resistive normal force, stemming from the piezoelectric sheets to oppose this deformation, is labeled as F_2 at each of the troughs. The Equations (1)–(4) [20] and variables from Tables 1 and 2 are used to perform an analytical analysis of the PEH. The force schematic is provided in Figure 7.

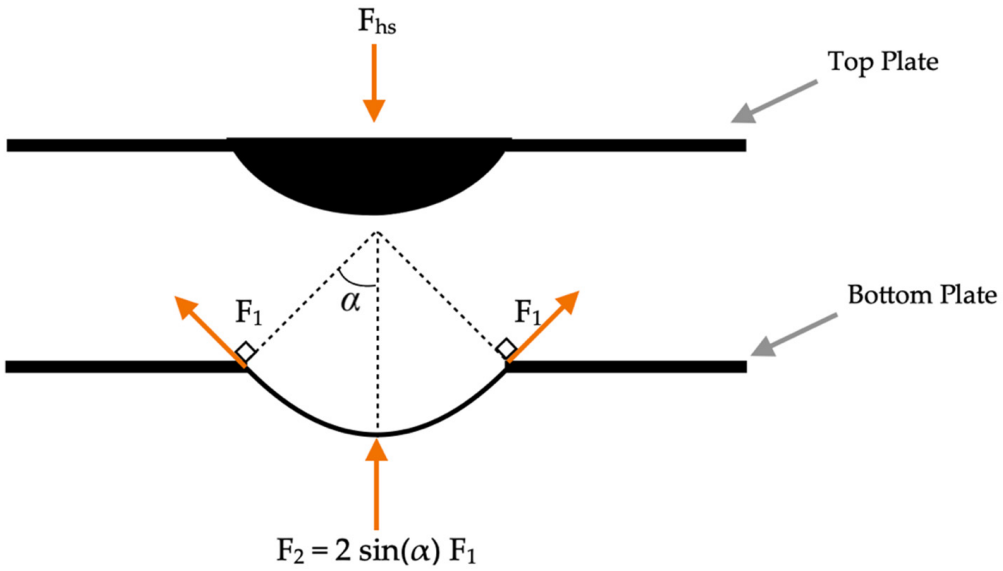

Figure 7. Energy-harvester assembly-force schematic diagram.

The force F_1 can be expressed as:

$$F_1 = A_{cs} N \sigma_c \tag{1}$$

where the compressive stress σ_c can be expressed using the normal strain ε as:

$$\sigma_c = Y\varepsilon \tag{2}$$

which leads into the approximation for the normal strain ε, which can be expressed as:

$$\varepsilon \approx \frac{\left[\frac{\alpha L}{\sin(\alpha)}\left(\frac{l}{L}\right)\right]}{l} = \frac{\alpha}{\sin(\alpha)} - 1 \tag{3}$$

As a further assumption, the surface friction between the PVDF sheets and the top/bottom plates is ignored; moreover, any compliance or damping in the shoe sole or the heel of the user is also ignored and assumed to be rigid-body interactions. It must be noted that the amount of charge generated by the PVDF sheets, whilst the top plate is pushed down via the F_{hs}, is equivalent to the charge generated when the F_{hs} is lifted and the collective resistive forces push the top plate to its starting position. For ease of calculation, is assumed that the force is equally distributed along the PVDF surface area, when in contact with the top and bottom plates. The accumulated charge (Q) on the surface can be calculated by the piezoelectric effect, using the following equation:

$$Q = N\left[d_{31}\sigma_c A_{cs}\frac{l}{h}\right] \approx N d_{31} A_{cs}\left[\frac{\alpha}{\sin(\alpha)} - 1\right]Y \tag{4}$$

Using Expressions (1)–(4) [20] and the data from the oscilloscope, the accumulated charge was deemed to be 65.25 µC/step, leading to a mean power generation of 3.80 mW/step during a regular gait cycle. At the cost of durability, the peak power generated during the stomping motion was substantially higher at 10.76 mW/step, although small signs of plastic deformation were visible after multiple attempts. There is a clear trade-off between the performance of the system and the reliability, depending on the severity of the input force.

3.3. Simulation Results

To best understand the behavior of the system under its operating loading conditions, COMSOL Multiphysics® was used to model the PEH. The assumptions used to model the system are as follows:

(1) The piezoelectric sheet is fixed at both ends;
(2) The surface is divided into sections representing the width of the crests/troughs;
(3) Uniform loading is applied to all of those sections and the crest/trough geometry of the top and bottom plate, which results in a gradient of the input force is ignored;
(4) The friction between the plates and the piezoelectric sheet is omitted.

Figure 8 depicts the 3D COMSOL Multiphysics® model, with the top face being the positive terminal, and the bottom face being the ground terminal. As can be seen, the surface is divided into sections, with red sections representing the compressive-force input from the top plate and with the grey sections representing the compressive normal force originating from the bottom plate.

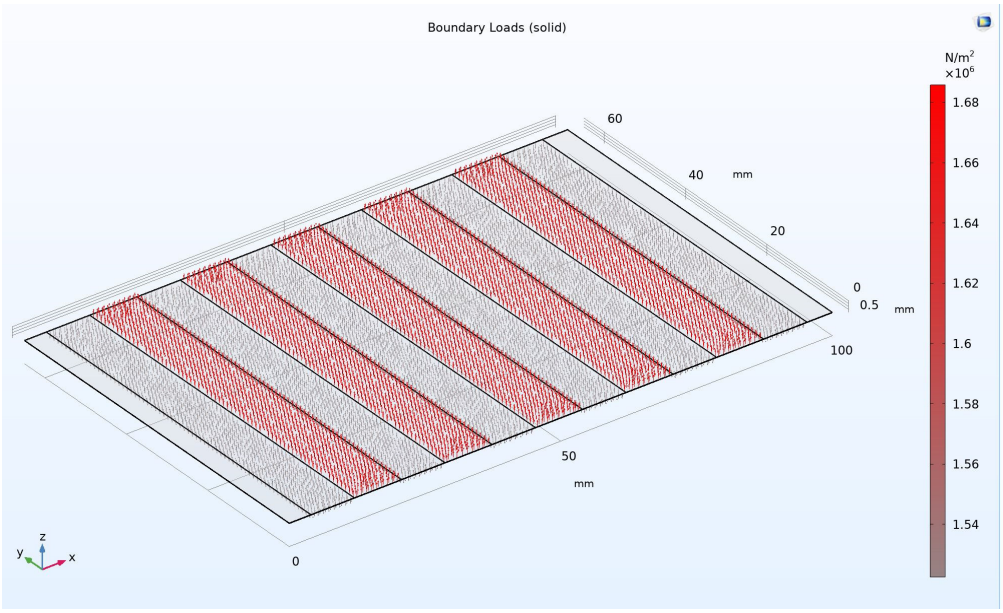

Figure 8. Boundary load simulation on COMSOL®.

The model meshing was performed using 287,145 tetrahedral elements. Under a distributed and uniform loading condition of 950 N, representing the weight of a 97 kg user stepping on the piezoelectric sheets, a deformation of +/−3mm in the positive/negative Z-direction is expected. Figure 9 depicts the resulting deformation under the given loading condition.

The deformation pattern closely resembles the experimental observations, although the dome-shaped deformation of the physical prototype is not being observed in the simulation results, due to the aforementioned assumptions.

Next, a simulation was performed to visualize the potential difference on the surface of the piezoelectric sheets. Figure 10 showcases the results and as expected, the areas that undergo the maximum stress and strain also lead to the highest potential differences. Thus, the sharp edges between the top and bottom plate are the areas of highest stress concentration and also peak voltage generation. A peak-to-peak voltage of 265 V is observed in the simulation study, although the stress and strain imposed on the outer edges of each section are more severe compared to the experimental prototype.

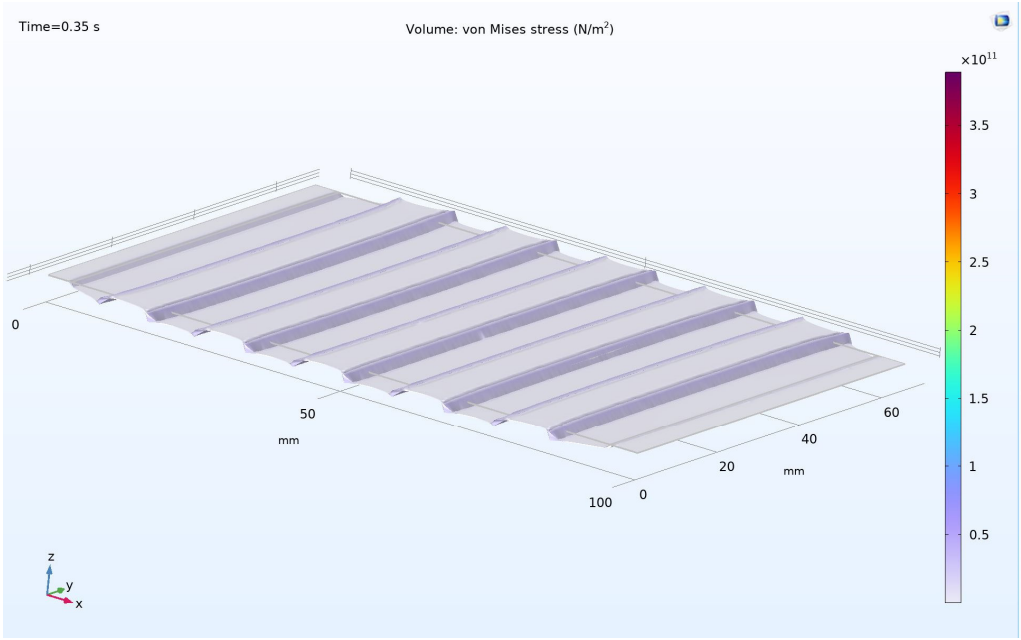

Figure 9. Von Mises stress (Pa) and deformation simulation on COMSOL®.

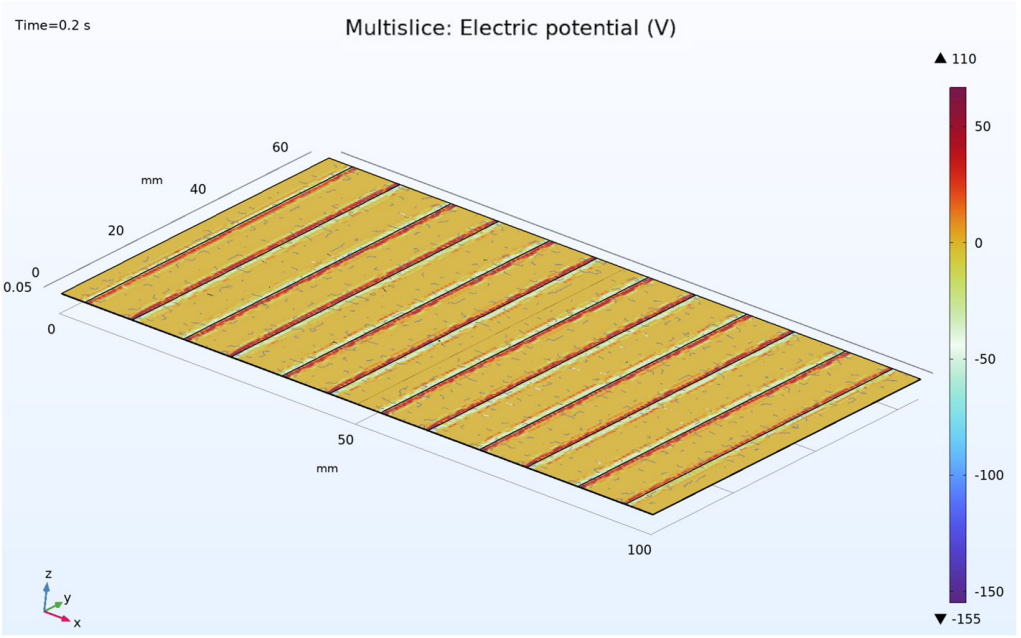

Figure 10. Electric potential (V) simulation on COMSOL®.

The data generated from the COMSOL Multiphysics® simulations were used to plot the power and voltage curves in a transient study over three seconds, representing several steps on the piezoelectric sheets. Showcased in Figure 11 are the voltage and displacement plotted during the time-dependent study. In addition, as showcased in Figure 11, the repeatable and comparable voltage readings are generated with each step, ranging from the +110 V to −155 V.

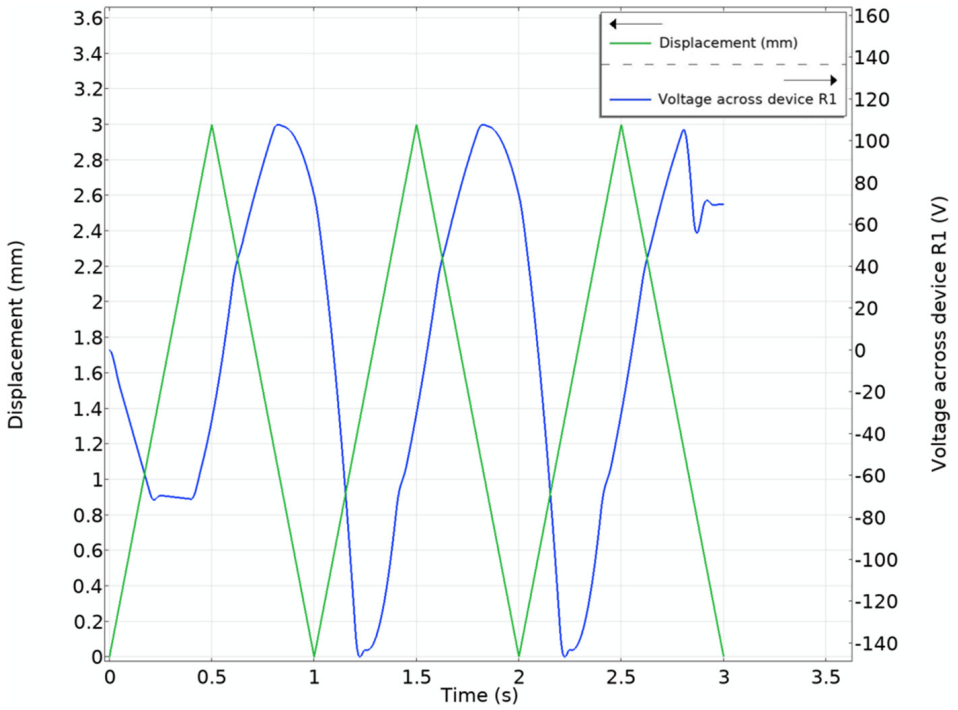

Figure 11. Time-dependent displacement (mm) and voltage (V) simulation on COMSOL®.

To assess the feasibility of this PEH, however, the power that can be generated must be determined by terminating the circuit with a matched resistor. Figure 12 plots the voltage (V) and power (mW) readings across the time-dependent study, spanning three seconds.

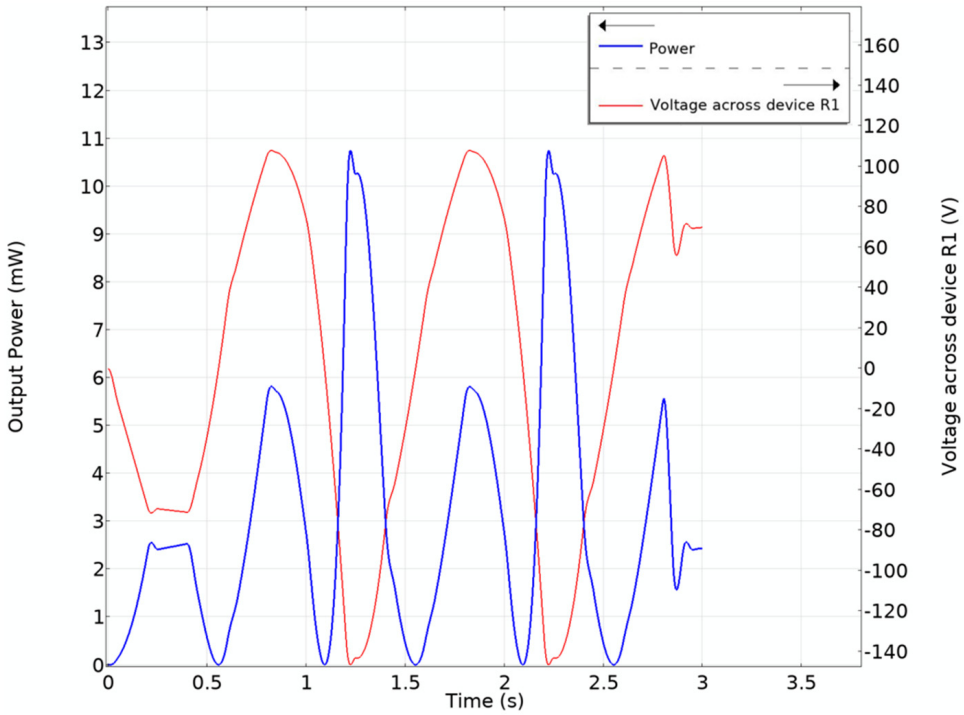

Figure 12. Time-dependent power (mW) and voltage (V) simulation on COMSOL®.

The peak power generated by the piezoelectric sheet is just under 11 mW/step, which closely matches the mathematical calculations.

4. Discussion

The finalized prototype performed as intended to serve the purpose of this research activity, meaning the PEH could harvest, store, and deploy energy as designed. Given the power-generation capabilities of the PEH and the demanding nature of the chosen application, it should be stated in a practical sense: the device would have to rely on an external power source for charging its battery. Using the device as a means of prolonging the usable duration of a charged battery, however, is a very promising and feasible spectacle for the prototype. Although power generation could be improved by increasing the number of PVDF layers, the resulting increase in thickness would impede the amount of deformation that can be achieved; thus requiring a larger assembly housing which hinders the form factor and, therefore, makes it not suitable for implementation inside a shoe sole. With the PEH generating 65.25 µC/step and assuming the battery capacity is 60 mAh, the number of steps required to fully charge a depleted battery is:

$$\frac{60\ mAh * 3600\ s}{65.25\ \mu C/step} = 3,310,344\ steps = \frac{3,310,344\ (steps)}{10,000\ (avg.steps/day)} \approx 331\ days \quad (5)$$

As the above calculation suggests, 331 days is not a very practical charging time for a fully depleted battery. When the device is used as merely a recharging mechanism for the system's battery whilst the device is in operation, 33 days of operation are able to charge 10% of the battery capacity, which resembles a more practical use of the PEH.

$$\frac{6\ mAh * 3600\ s}{65.25\ \mu C/step} = 331,034\ steps = \frac{331,034\ steps}{10,000\ (avg.steps/day)} \approx 33\ days \quad (6)$$

For improved power generation, two PEHs can be worn (one in each shoe) and whilst one is generating electrical energy and deploying it to the desired muscle, the other unit in the healthy foot can recharge its battery with each step. The units would then be swapped when the charge depletes on the PEH worn on the hemiplegic foot. This would reduce the overall charge-generation time by half and reduce its dependence on an external power source. Deploying this strategy would cut the recharge time in half, to approximately 16.5 days.

$$\frac{6\ mAh * 3600\ s}{65.25\ \mu C/step} = 331,034\ steps = \frac{331,034\ steps}{20,000\ (avg.steps/day)} \approx 16.5\ days \quad (7)$$

The device in its current state is fully capable of powering sensors, such as a sensor for blood pressure, a meter for glucose meter, or activity trackers [22]. For future steps, stimulating smaller muscles could be an area of interest where muscle contraction is not really required, yet low levels of stimulation would suffice and be of medical benefit for a patient. Focusing on smaller muscles would alleviate the need for a high-capacity battery, thus making the PEH more practical. For example, recharging 10% of a 10mAh capacity battery would require just under 3 days of use and still be capable of powering certain medical devices.

5. Conclusions

The findings of this research activity provided a solid baseline for the feasibility of a shoe-mounted PEH and performed experimental, mathematical, and simulation analyses on the prototype. Improvements can be made by packaging the circuitry in a convenient form, to allow the PEH to be comfortably worn by the user. This PEH proved to be fully capable of powering sensors, such blood pressure sensors, glucose meters, or activity trackers, whilst also being effective at stimulating smaller muscles. For more demanding applications such as stimulating the TA muscle, the PEH would have to rely on battery charging via an external power source, but it can be effective as a recharging mechanism to reduce the dependence on external power sources. Although FES and PEH technology

will continue to evolve, we have successfully bridged the gap that we set out to investigate with our PEH system, to deliver muscle stimulation safely and efficaciously.

Author Contributions: K.B. and P.S. initiated this research exercise to investigate novel applications of EHs in the biomedical field. The contributions of P.S. included initial-concept generation and methodology, modeling of the system, material and prototype fabrication, testing, data curation, and validation. G.P. designed the entire electrical circuitry for the research project as well as validated the voltage and power outputs from the prototype. G.P. also offered guidance in the fabrication steps of the electrical components and investigated and validated the results. The contributions of M.S. were focused on initial conceptualization steps and finding a suitable biomedical application of the EH. Biomedical application of the harvested energy was part of M.S.'s contribution. K.B. offered guidance and mentorship throughout the course of this research project and supervised the progress whilst also acquiring the necessary funding. The original-draft preparation along with the editing and review steps were undertaken by P.S., G.P. and M.S. All authors have read and agreed to the published version of the manuscript.

Funding: This research was funded by the Connaught Global Challenge Award program.

Data Availability Statement: Not applicable.

Acknowledgments: This research was funded by the Connaught Global Challenge Award study. The authors also acknowledge S. Ranjan Mishra and Christopher Hu for their guidance in the COMSOL Multiphysics® computer simulations presented in this paper.

Conflicts of Interest: The authors declare no conflict of interest. The funders had no role in the design of the study; in the collection, analyses, or interpretation of data; in the writing of the manuscript; or in the decision to publish the results.

References

1. Alam, M.; Li, S.; Ahmed, R.U.; Yam, Y.M.; Thakur, S.; Wang, X.Y.; Tang, D.; Ng, S.; Zheng, Y.P. Development of a battery-free ultrasonically powered functional electrical stimulator for movement restoration after paralyzing spinal cord injury. *J. Neuroeng. Rehabil.* **2019**, *16*, 36. [CrossRef] [PubMed]
2. Carolus, A.E.; Becker, M.; Cuny, J.; Smektala, R.; Schmieder, K.; Brenke, C. The interdisciplinary management of foot drop. *Dtsch. Ärztebl. Int.* **2019**, *116*, 347. [CrossRef] [PubMed]
3. Sabut, S.K.; Sikdar, C.; Kumar, R.; Mahadevappa, M. Functional electrical stimulation of dorsiflexor muscle: Effects on dorsiflexor strength, plantarflexor spasticity, and motor recovery in stroke patients. *NeuroRehabilitation* **2011**, *29*, 393–400. [CrossRef] [PubMed]
4. Karniel, N.; Raveh, E.; Schwartz, I.; Portnoy, S. Functional electrical stimulation compared with ankle-foot orthosis in subacute post stroke patients with foot drop: A pilot study. *Assist. Technol. Off. J. RESNA* **2021**, *33*, 9–16. [CrossRef] [PubMed]
5. Kim, K.-B.; Jang, W.; Cho, J.Y.; Woo, S.B.; Jeon, D.H.; Ahn, J.H.; Do Hong, S.; Koo, H.Y.; Sung, T.H. Transparent and flexible piezoelectric sensor for detecting human movement with a boron nitride nanosheet (BNNS). *Nano Energy* **2018**, *54*, 91–98. [CrossRef]
6. Zurbuchen, A.; Pfenniger, A.; Stahel, A.; Stoeck, C.T.; Vandenberghe, S.; Koch, V.M.; Vogel, R. Energy Harvesting from the Beating Heart by a Mass Imbalance Oscillation Generator. *Ann. Biomed. Eng.* **2013**, *41*, 131–141. [CrossRef] [PubMed]
7. Hinchet, R.; Yoon, H.-J.; Ryu, H.; Kim, M.-K.; Choi, E.-K.; Kim, D.-S.; Kim, S.-W. Transcutaneous ultrasound energy harvesting using capacitive triboelectric technology. *Science* **2019**, *365*, 491–494. [CrossRef] [PubMed]
8. Jeong, S.Y.; Xu, L.L.; Ryu, C.H.; Kumar, A.; Do Hong, S.; Jeon, D.H.; Cho, J.Y.; Ahn, J.H.; Joo, Y.H.; Jeong, I.W.; et al. Wearable Shoe-Mounted Piezoelectric Energy Harvester for a Self-Powered Wireless Communication System. *Energies* **2021**, *15*, 237. [CrossRef]
9. Yin, Z.; Gao, S.; Jin, L.; Guo, S.; Wu, Q.; Li, Z. A shoe-mounted frequency up-converted piezoelectric energy harvester. *Sens. Actuators A Phys.* **2021**, *318*, 112530. [CrossRef]
10. Fan, K.; Liu, Z.; Liu, H.; Wang, L.; Zhu, Y.; Yu, B. Scavenging energy from human walking through a shoe-mounted piezoelectric harvester. *Appl. Phys. Lett.* **2017**, *110*, 143902. [CrossRef]
11. Narolia, T.; Gupta, V.K.; Parinov, I.A. Design and analysis of a shear mode piezoelectric energy harvester for rotational motion system. *J. Adv. Dielectr.* **2020**, *10*, 2050008. [CrossRef]
12. Manan, A.; Rehman, M.U.; Ullah, A.; Ahmad, A.S.; Iqbal, Y.; Qazi, I.; Khan, M.A.; Shah, H.U.; Wazir, A.H. High energy storage density with ultra-high efficiency and fast charging–discharging capability of sodium bismuth niobate lead-free ceramics. *J. Adv. Dielectr.* **2021**, *11*, 2150018. [CrossRef]
13. Chebanenko, V.A.; Zhilyaev, I.V.; Soloviev, A.N.; Cherpakov, A.V.; Parinov, I.A. Numerical optimization of the piezoelectric generators. *J. Adv. Dielectr.* **2020**, *10*, 2060016. [CrossRef]

14. Shendkar, C.; Lenka, P.K.; Biswas, A.; Kumar, R.; Mahadevappa, M. Design and Development of A Low-Cost Biphasic Charge-Balanced Functional Electric Stimulator and Its Clinical Validation. *Healthc. Technol. Lett.* **2015**, *2*, 129–134. Available online: https://ietresearch.onlinelibrary.wiley.com/doi/10.1049/htl.2015.0001 (accessed on 6 December 2021). [CrossRef] [PubMed]
15. Chen, C.F.; Chen, W.S.; Chou, L.W.; Chang, Y.J.; Chen, S.C.; Kuo, T.S.; Lai, J.S. Pulse Energy as A Reliable Reference for Twitch Forces Induced by Transcutaneous Neuromuscular Electrical Stimulation. *IEEE Trans. Neural Syst. Rehabil. Eng.* **2012**, *20*, 574–583. Available online: https://ieeexplore.ieee.org/document/6177269 (accessed on 23 January 2022). [CrossRef] [PubMed]
16. Cheng, K.E.; Lu, Y.; Tong, K.Y.; Rad, A.B.; Chow, D.H.; Sutanto, D. Development of A Circuit for Functional Electrical Stimulation. *IEEE Trans. Neural Syst. Rehabil. Eng.* **2004**, *12*, 43–47. [CrossRef] [PubMed]
17. Dickinson, D. Piezoelectric Energy Harvesting Power Supply. Analog Devices. 2010. Available online: https://www.analog.com/en/about-adi/news-room/press-releases/2010/piezoelectric-energy-harvesting-power-supply.html (accessed on 5 March 2022).
18. DC1459B Evaluation Kit-Analog Devices. Analog.Com. Available online: https://www.analog.com/media/en/technical-documentation/user-guides/dc1459B.pdf (accessed on 7 March 2022).
19. Falin, J. Coupled Inductors Broaden DC/DC Converter Usage. 2010. Available online: https://www.ti.com/lit/an/slyt380/slyt380.pdf (accessed on 12 March 2022).
20. Zhao, J.; You, Z. A shoe-embedded piezoelectric energy harvester for wearable sensors. *Sensors* **2014**, *14*, 12497–12510. [CrossRef] [PubMed]
21. Piezo Sheet PVDF Film with 100 nm Thick Aluminum Electrode. Piezoelectric & Pyroelectric PVDF & PVDF-TrFE, Resin, Film, Sensor, Transducer, and Test Instrument. (n.d.). Retrieved 24 April 2022. Available online: https://piezopvdf.com/Aluminium-piezo-sheet-pvdf-film-45um-120um/ (accessed on 28 March 2022).
22. Chen, W.; Sonntag, C.; Boesten, F.; Oetomo, S.B.; Feijs, L. A design of power supply for neonatal monitoring with wearable sensors. *J. Ambient. Intell. Smart Environ.* **2009**, *1*, 185–196. [CrossRef]